Uranium ferromagnet with negligible magnetocrystalline anisotropy: $U_4Ru_7Ge_6$

Michal Vališka,* Martin Diviš, and Vladimír Sechovský
Faculty of Mathematics and Physics, Charles University, DCMP, Ke Karlovu 5, CZ-12116 Praha 2, Czech Republic
(Received 22 November 2016; revised manuscript received 4 February 2017; published 27 February 2017)

Strong magnetocrystalline anisotropy (MA) is a well-known property of uranium compounds. The almost isotropic ferromagnetism in $U_4Ru_7Ge_6$ reported in this paper represents a striking exception. We present results for magnetization, ac susceptibility, thermal expansion, specific heat, and electrical resistivity measurements performed on a $U_4Ru_7Ge_6$ single crystal at various temperatures and magnetic fields; we discuss the results in relation to first-principles electronic structure calculations. $U_4Ru_7Ge_6$ behaves as an itinerant $5f$-electron ferromagnet ($T_C = 10.7$ K, $\mu_S = 0.85\,\mu_B$/f.u. at 1.9 K). The ground-state easy magnetization direction is along the [111] axis of the cubic lattice. The anisotropy field $\mu_0 H_a$ along the [001] direction is only about 0.3 T, which is at least three orders of magnitude smaller than for other U ferromagnets. At $T_r = 5.9$ K the easy magnetization direction changes to [001], and remains [001] up to T_C. This transition is due to a change in magnetic symmetry, and is quite apparent in the low-field magnetization, ac susceptibility, and thermal expansion data, whereas only weak anomalies are observed at T_r in the temperature dependence of the specific heat and electrical resistivity. The magnetoelastic interaction induces a rhombohedral (tetragonal) distortion of the paramagnetic cubic crystal lattice in the case of the [111] ([001]) easy magnetization direction. The rhombohedral distortion is connected with two crystallographically inequivalent U sites. Our density functional theory calculations, including spin-orbit interaction (SOI) of the U $5f$ electrons, also produces two inequivalent U sites, because SOI leads to a reduction of the symmetry of the former cubic structure. The calculated ground state is in agreement with the experimentally observed [111] easy magnetization direction. The first excited state has moments along the [001] direction, which agrees with the moment orientation for $T > T_r$. The energy of the first excited state is 0.9 meV above the ground state, which is comparable to the value of 0.51 meV, corresponding to $k_B T_r$. We propose that weak MA of the $U_4Ru_7Ge_6$ compound is due to the lack of direct overlap of the $5f$ orbitals of the nearest U ions, which is screened out by the closed Ru and Ge cuboctahedra coordinating each U ion.

DOI: 10.1103/PhysRevB.95.085142

I. INTRODUCTION

Magnetocrystalline anisotropy (MA) is manifested by locking the magnetic moments in a specific orientation (usually the easy magnetization direction) with respect to the crystal axes. A quantitative measure of MA, the anisotropy field H_a, is the magnetic field needed to be applied in the hard magnetization direction in order to reach the easy axis magnetization value. The key prerequisites of MA are the orbital moment of a magnetic ion, the spin-orbit interaction (SOI) coupling the orbital and spin moment, and interactions with neighboring ions [1,2]. The SOI is a relativistic effect, and becomes stronger in heavier atoms. Consequently MA dominates magnetism in materials with lanthanide and actinide series ions bearing magnetic moments of the $4f$ and $5f$ electrons, respectively.

The widely accepted scenario of the origin of MA involves the crystal electric-field (CEF) interaction, the single-ion mechanism born in the electrostatic interaction of the anisotropic crystalline electric field (the potential created at the magnetic ion site by the electric charge distribution in the rest of the crystal) with the aspherical charge cloud of the magnetic electrons. The electron orbital adopts the direction that minimizes the CEF interaction energy. The single-ion anisotropy is most often encountered in compounds with lanthanide series ions having well-localized $4f$ electrons [3,4].

Contrary to the $4f$ orbitals deeply buried in the core electron density of lanthanide series ions, the spatially extended uranium $5f$-electron wave functions interact with the overlapping $5f$ orbitals of the nearest-neighbor U ions ($5f$-$5f$ overlap) as well as with the valence electron orbitals of ligands ($5f$-ligand hybridization [5]). Consequently the $5f$-electron wave functions lose the atomic character and simultaneously the U magnetic moments become reduced. This reduction is in spite of the fact that the strong spin-orbit coupling induces a predominant orbital magnetic moment antiparallel to the spin moment in the spin-polarized $5f$-electron energy bands. This effect was first demonstrated for the itinerant $5f$-electron magnetism in UN [6]. In some cases very small, or even zero, total magnetic moment of a U ion is observed as a result of mutual compensation of the antiparallel spin and the orbital component. The itinerant $5f$-electron ferromagnet UNi_2 [7], with the U magnetic moment of a few hundredths of μ_B, serves as an excellent example as documented by results of polarized neutron measurements [8] and first-principles electronic structure calculations [9]. Despite the itinerant character of the magnetism, UNi_2 exhibits a very strong MA, with $\mu_0 H_a \gg 35$ T at 4.2 K [10].

The very strong MA seems to be inherent to the uranium magnetism. The typical values of the MA field of most uranium intermetallic compounds are of the order of hundreds Tesla [11]. The strong anisotropy is also reported for the cubic U pnictides and chalcogenides [12,13].

The strong interaction of the spatially extended U $5f$ orbitals with surrounding ligands in the crystal and participation of $5f$ electrons in bonding [14,15] imply an essentially different mechanism of MA based on a two-ion (U-U) interaction. The anisotropy of the bonding and $5f$-ligand

*michal.valiska@gmail.com

hybridization assisted by the strong SOI are the key ingredients of the two-ion anisotropy in 5f-electron magnets.

The systematic occurrence of particular types of anisotropy related to the layout of the U ions in a crystal lattice suggests, in materials in which the U-U co-ordination is clearly defined in the crystal structure, the easy magnetization direction is in the plane perpendicular to the nearest U-U links [11,16]. This scenario, however, does not hold for crystal structures in which the direct U-U link is shielded by the presence of non-U ligands between nearest U neighbors. Cooper *et al.* [17,18] have formulated a relatively simple model of the two-ion interaction. This model, leading to qualitatively realistic results, is based on the Coqblin-Schrieffer approach to the mixing of ionic f states and conduction-electron states, in which the mixing term of the Hamiltonian of Anderson type is treated as a perturbation, and the hybridization interaction is replaced by an effective f-electron-band electron resonant exchange scattering. The theory has been further extended so each partially delocalized f-electron ion is coupled by the hybridization to the band electron sea, leading to a hybridization-mediated anisotropic two-ion interaction giving an anisotropic magnetic ordering.

In this paper we focus on magnetism in the $U_4Ru_7Ge_6$ compound. Although the first $U_4Ru_7Ge_6$ single crystals were grown already in the late 1980's, only a vague report on ferromagnetism ($T_C \sim 7$ K, 0.2 μ_B/U ion in 5 T at 4.3 K) [19] and no information on anisotropy can be found in literature. Therefore we have grown a high-quality single crystal of this compound and measured its magnetization, ac susceptibility, thermal expansion, specific heat, and electrical resistivity with respect to temperature and magnetic field. A weakly anisotropic ferromagnetism has been observed below $T_C = 10.7$ K. The ferromagnetic ground state is characterized by the easy magnetization axis along the [111] crystallographic direction. A magnetic phase transition at which the easy magnetization axis changes from [111] to [001] is observed at $T_r = 5.9$ K. The [111] ([001]) phase is associated with a tiny rhombohedral (tetragonal) distortion of the paramagnetic cubic crystal structure hardly observable in x-ray-diffraction measurements. Here we demonstrate that it can be indicated by thermal-expansion data. To shed more light on the microscopic mechanisms responsible for the unusual $U_4Ru_7Ge_6$ magnetism we also performed first-principles electronic structure calculations.

II. EXPERIMENTAL DETAILS

The $U_4Ru_7Ge_6$ single crystal has been grown by the Czochralski method in a tri-arc furnace from constituent elements (purity of Ru 3N5 and Ge 6N). The uranium metal was purified using the solid state electrotransport technique. Half of the crystal was wrapped in the Ta foil (purity 4N), sealed in a quartz tube under the vacuum of 1×10^{-6} mbar, and subsequently annealed at 1000 °C for 7 days. The high quality of both crystals was verified by Laue diffraction using a Photonic Science X-Ray Laue system with a CCD camera and single-crystal x-ray diffraction on a Rigaku R-Axis Rapid II diffractometer with a Mo anode. Both the as-cast and annealed single crystal were pulverized and characterized by x-ray powder diffraction (XRPD) at room temperature on a Bruker D8 Advance diffractometer with a Cu anode. The XRPD data were evaluated by the Rietveld technique [20] using FULLPROF/WINPLOTR software [21,22]. The chemical composition of each single crystal was verified by a scanning electron microscope Tescan Mira I LMH equipped with an energy dispersive x-ray (EDX) detector Bruker AXS. Samples for individual experiments were cut from the annealed crystal with a fine wire saw to prevent induction of additional stresses and lattice defects.

The magnetization (in a magnetic field up to 7 T applied along the [001] or [111] directions) and ac susceptibility (the ac magnetic field with the amplitude of 300 μT applied along [001]) were measured by a Quantum Design Magnetic Property Measurement System (MPMS) superconducting quantum interference device magnetometer in the temperature range from 1.9 to 300 K. The magnetization along [111] was measured up to 14 T by a Quantum Design Physical Property Measurement System (PPMS) device equipped with a vibrating sample magnetometer. Specific-heat data were collected by the thermal relaxation technique in the temperature range from 0.4 to 20 K in magnetic fields up to 9 T by a Quantum Design PPMS device. The electrical resistivity measurements were realized using the ac transport option of the Quantum Design PPMS instrument with ac current applied along [001] or [111] in the temperature range from 1.9 to 300 K. Thermal expansion measurements along the [100], [001], and [111] directions were made in the temperature range from 1.9 to 30 K using a miniature capacitance dilatometer [23] implemented in the Quantum Design PPMS device. All the instruments mentioned above are a part of the Charles University Magnetism and Low Temperature Laboratories (MLTL, see http://mltl.eu/).

III. RESULTS

A. Crystal structure and chemical composition

The Rietveld refinement of our XRPD data collected on both the pulverized as-cast and annealed single crystal confirmed previous reports [19,24,25] that $U_4Ru_7Ge_6$ possesses at room temperature a cubic crystal structure of the $Im\bar{3}m$ space group (see Fig. 1). The room-temperature powder pattern is plotted in Fig. 2. The corresponding lattice parameters (see Table I) determined for both the as-cast and annealed crystal are nearly identical. The coordination of the U atoms in the $U_4Ru_7Ge_6$ structure is a slightly distorted cuboctahedron [26], and the U − Ru_1 distance (2.932 Å) is shorter than the closest U − U distance (4.147 Å).

Elemental mapping by EDX confirmed homogeneity of all the studied samples. The average of multiple point scans from the different parts of the sample gave the resulting stoichiometry 4.4(4):6.9(2):5.7(1), pointing to a slight Ge deficiency.

B. Low-temperature magnetization

The magnetization curves $M(\mu_0 H)$ measured in a magnetic field, applied along either the [001] or [111] direction document that $U_4Ru_7Ge_6$ is at 1.9 K ferromagnetic with the easy magnetization direction along the [111] axis (see Fig. 3). The spontaneous magnetization is $M_{S[111]} = 0.88(1)\,\mu_B$ [obtained as an extrapolation of the $M_{[111]}(\mu_0 H)$ dependence to $\mu_0 H =$

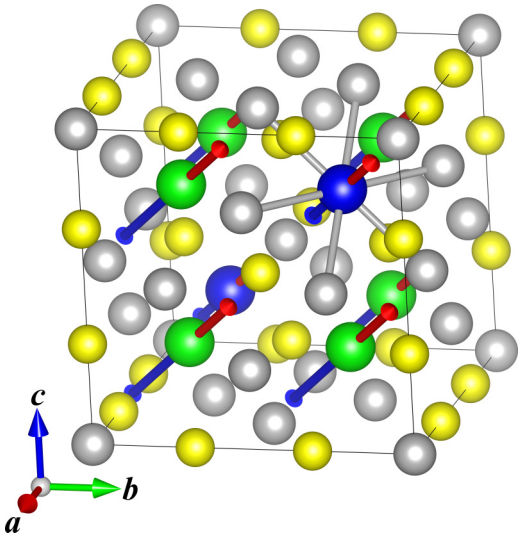

FIG. 1. Structure of $U_4Ru_7Ge_6$ together with magnetic moments from theoretical calculations. Arrows for magnetic moments are in proper relative scale but in arbitrary units. U_1 ions are blue, U_2 are green, Ru_1 and Ru_2 are gray, and Ge are yellow. The shortest distances $U_{(1,2)} - Ru_1$ are marked by gray cylinders.

0 T]. The spontaneous magnetization value along the [001] direction is lower, $M_{S[001]} = 0.51(1)\,\mu_B$. This value is in very good agreement with the Néel phase law [27] for a cubic system. It proposes that $M_{S[001]}$ can be obtained from the $M_{S[111]}$ value multiplied by the appropriate direction cosine, i.e., $M_{S[001]} = \sqrt{\frac{1}{3}} M_{S[111]}$. For fields higher than 0.3 T the $M_{[111]}(\mu_0 H)$ and $M_{[001]}(\mu_0 H)$ curves merge (we estimate the $\mu_0 H_a$ value to be 300 mT). However, the magnetization does not saturate in a field up to 14 T, where the magnetization reaches the value of $1.4\,\mu_B$/f.u. The poor saturation of the magnetization in high magnetic fields is typical for itinerant electron ferromagnets. The increasing magnetic moment with increasing magnetic field is then reflecting the magnetic-field

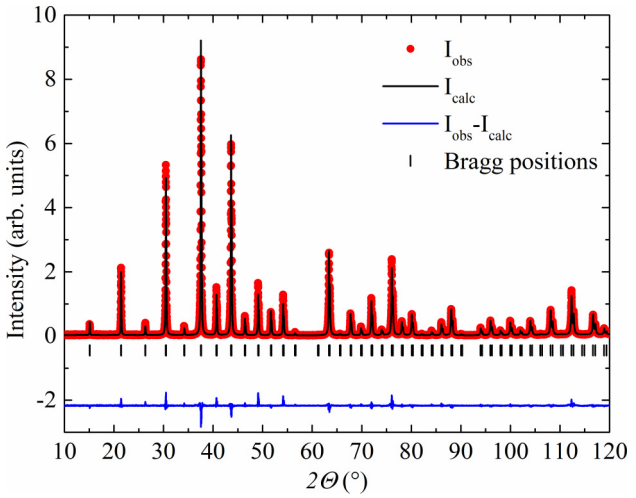

FIG. 2. X-ray powder-diffraction pattern of an as-cast pulverized $U_4Ru_7Ge_6$ single crystal measured at room temperature.

TABLE I. Results of structure analysis at room temperature.

Space group $Im\bar{3}m$	As cast	Annealed
a	8.2934(2) Å	8.2933(3) Å
$U(x,y,z)$, $8c$	(0.25, 0.25, 0.25)	(0.25, 0.25, 0.25)
$Ru_1(x,y,z)$, $12d$	(0.25, 0, 0.5)	(0.25, 0, 0.5)
$Ru_2(x,y,z)$, $2a$	(0, 0, 0)	(0, 0, 0)
$Ge(x,y,z)$, $12e$	(0.31375(13), 0, 0)	(0.31360(11), 0, 0)

induced change of the electronic structure (additional splitting of the majority and minority subbands).

The observed very weak magnetization anisotropy makes $U_4Ru_7Ge_6$ a unique exception among the U ferromagnets, which are normally strongly anisotropic with anisotropy fields of several hundred Tesla [11]. In the next section we approach this issue by first-principles electronic structure calculations focused on the microscopic origin of U magnetic moments and MA.

C. First-principles calculations

To obtain microscopic information about magnetism in $U_4Ru_7Ge_6$ we applied the first-principles methods based on density functional theory including SOI. The Kohn-Sham-Dirac four-component equations have been solved by using the latest version of the full-potential-local-orbitals computer code [28]. We have used both the local spin density approximation (LSDA) [29] and the general gradient approximation (GGA) [30]. The $5f$ states were treated as itinerant Bloch states. Several k meshes in the Brillouin zone were involved to ensure the convergence of charge densities, total energy, and magnetic moments. For the sake of simplicity we assumed a collinear ferromagnetic structure. In $U_4Ru_7Ge_6$ the total ground-state magnetic moment was found to point along the [111] direction. Due to the SOI, the symmetry is reduced from 48 to 12 symmetry operations. Instead of four symmetrically equivalent U ion sites in the scalar relativistic treatment with a spin-only magnetic moment, we have the spin and orbital angular momenta coupled by the relativistic SOI which divides the U ions in two subgroups consistent with the expected rhombohedral distortion induced by magnetoelastic interaction in the case of the [111] easy magnetization direction. The U ions in the first subgroup at the U_1 positions (0.25, 0.25, 0.25) and (0.75, 0.75, 0.75) have a very small total magnetic moment of $0.01\,\mu_B$ due to cancellation of the almost equal-size antiparallel spin and orbital moment (see Fig. 1), using LSDA. In GGA, the cancellation is not so pronounced leading to the moment of $0.103\,\mu_B$. The second subgroup includes the U ions at the remaining six U_2 positions bearing the spin magnetic moment of $-0.56\,\mu_B$ and the orbital magnetic moment of

TABLE II. Results of the modified Curie-Weiss fit in the temperature interval 30–300 K.

$B \parallel$	μ_{eff} (μ_B/U)	θ_P (K)	$\chi_0 \times 10^{-8}$ (m^3 mol^{-1})
[001]	1.43	7.5	5.8
[111]	1.43	8.1	5.7

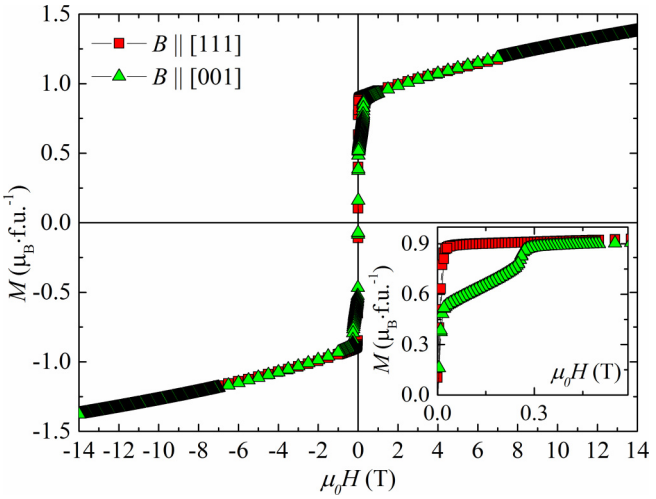

FIG. 3. Field dependence of magnetization isotherms of $U_4Ru_7Ge_6$ at 1.9 K for the applied magnetic field along the [111] and [001] directions. The inset shows a low-field detail.

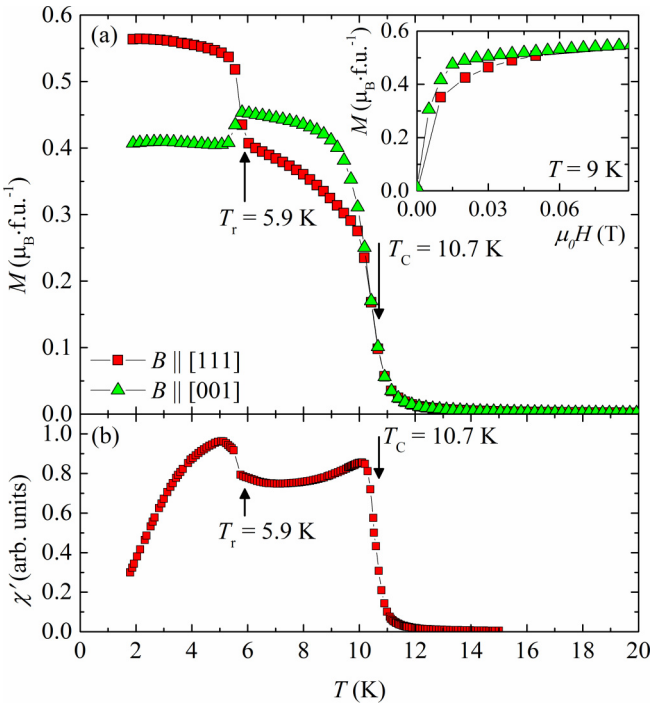

FIG. 4. Temperature dependence of the magnetization of $U_4Ru_7Ge_6$ measured in a magnetic field of 10 mT (in the ZFC regime) applied along the [111] or [001] direction (a) and temperature dependence of the ac susceptibility in the ac field applied along the [111] direction (b). The inset in the upper panel shows field dependence of magnetization at 9 K.

0.79 μ_B, using LSDA. GGA provides a slightly enhanced spin ($-0.82\,\mu_B$) and orbital ($1.021\,\mu_B$) magnetic moment. There are also some hybridization-induced Ru magnetic moments, which summed to give $0.29\,\mu_B$ and $0.604\,\mu_B$ for LSDA and GGA, respectively. The calculated Ge magnetic moment is negligible for both methods. The summation over the 17 ions (one formula unit) in the primitive crystallographic cell gives the total magnetic moment of $1.01\,\mu_B$ and $1.11\,\mu_B$ for LSDA and GGA, respectively. It is somewhat larger than the spontaneous magnetic moment determined by experiment.

We have also performed relativistic calculations with the moment along [001]. In this case the cubic symmetry is reduced to tetragonal, and all U moments have the same value of spin ($-0.529\,\mu_B$ and $-0.794\,\mu_B$) and orbital ($0.706\,\mu_B$ and $0.939\,\mu_B$) components for LSDA and GGA, respectively. The coordination polyhedra of the U atom contain seven Ru atoms with partially occupied delocalized Ru $4d$ states (see Fig. 1). These $4d$ states hybridized strongly with U $5f$ states. Therefore the correlations inside LSDA and GGA are sufficient for a good description of magnetic moments in the presence of spin-orbit coupling. It is not necessary to introduce some other method which would describe strong correlations between the $5f$ electrons like LSDA+U. This is, for instance, the main difference of the $U_4Ru_7Ge_6$ case from the heavy-fermion compound UBe_{13} [31], in which the uranium ion is buried in the Be-ligand cage, but the Be has an occupied $2s$ subshell and hybridization with U $5f$ states is much weaker. Therefore the correlations inside the $5f$ subshell are much more pronounced than in $U_4Ru_7Ge_6$.

When calculating the magnetocrystalline anisotropy energy between the configurations of magnetic moments aligned along the [111] and [001] axis, the values of the total energy were used. Our convergence tests have shown that the total energy from LSDA calculations is better converged than from GGA. Therefore, we used LSDA values for our final consideration. In agreement with experiment, we have found the ground state with the total moment pointing to the [111] direction using both LSDA and GGA. The excited state with the moment pointing to the [001] direction is 0.9 meV above the ground state. This value is in the order of magnitude in agreement with the energy corresponding to T_r, the temperature of the [111] to [001] spin reorientation transition.

D. Magnetization near the phase transitions

The Curie temperature, T_C, of a ferromagnet is frequently estimated as the temperature of the inflection point of the M versus T curve measured in a low magnetic field and/or of the temperature dependence of the ac susceptibility. In Fig. 4(a) one can see from $M(T)$ measured in the external magnetic field of 10 mT applied along the [111] or [001] direction, an inflection point at the same temperature of 10.6 ± 0.1 K ($\sim T_C$) and a crossing at $T_r = 5.9 \pm 0.1$ K. Two sharp anomalies at corresponding temperatures can be seen in the $\chi_{ac}(T)$ dependence shown in Fig. 4(b). These results clearly document that $U_4Ru_7Ge_6$ orders at T_C ferromagnetically with the easy magnetization axis [001] [which is demonstrated by the 9-K magnetization isotherms in the inset of Fig. 4(a)]. At T_r the crystal undergoes a spin reorientation transition to a ground state characterized by the easy magnetization axis along [111].

A method of determining Curie temperature of a ferromagnet from magnetization data is based on the analysis of Arrott plots (M^2 versus $\mu_0 H/M$) [32]. Linear Arrott plots are in fact a graphical representation of the Ginsburg-Landau mean field theory of magnetism in the vicinity of the ferromagnetic

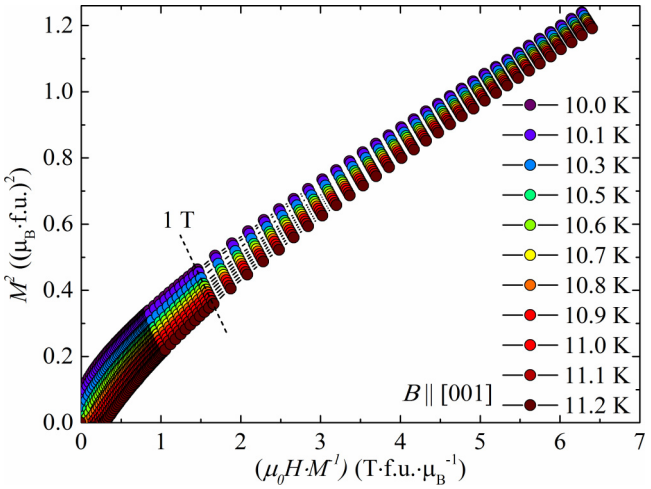

FIG. 5. Arrott plots for $U_4Ru_7Ge_6$ in a magnetic field applied along the [001] direction.

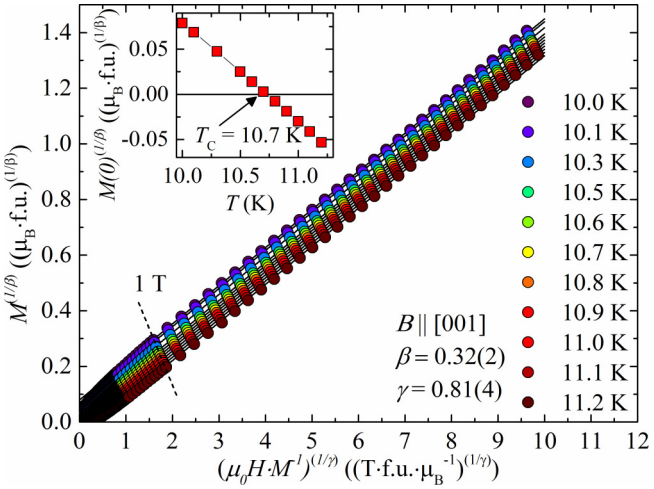

FIG. 6. Arrott-Noakes plots reflecting the equation of states (with $\beta = 0.31 \pm 0.03$ and $\gamma = 0.81 \pm 0.04$) for $U_4Ru_7Ge_6$ in the magnetic field applied along the [001] direction.

to paramagnetic second-order phase transition. In Fig. 5 one can see that the Arrott plots for $U_4Ru_7Ge_6$ in a magnetic field applied along the easy magnetization direction [001] are almost linear with varying slope for magnetic fields between 1 and 7 T, whereas for lower fields they became slightly convex. The linear extrapolations of high-field data to the vertical axis mark the values of M^2, which are considered as estimates of the square spontaneous magnetization M_S^2. The spontaneous magnetization as the order parameter of a ferromagnetic phase vanishes at T_C. Note the use of the linear extrapolations from high fields in the case of the convex curvature of $U_4Ru_7Ge_6$ Arrott plots in low fields leads to a certain overestimation of M_S values, and consequently to a higher estimated T_C value.

A more precise T_C value may be expected from the generalized approach using the Arrott-Noakes equation of state $(\mu_0 H/M)^{1/\gamma} = (T - T_C)/T_1 + (M/M_1)^{1/\beta}$, where M_1 and T_1 are material constants [33]. We reanalyzed our data by plotting them as $M^{1/\beta}$ versus $(\mu_0 H/M)^{1/\gamma}$ with β and γ values chosen to get the best possible linearity of these plots while keeping them parallel with constant slope. The values $\beta = 0.31 \pm 0.03$ and $\gamma = 0.81 \pm 0.04$ lead to a linear dependence in the broad field range, except the very low fields. This construction is plotted in Fig. 6 for all measured isotherms. This approach leads to $T_C = 10.7 \pm 0.1$ K (see inset of Fig. 6), in agreement with the estimated value from the low-field magnetization data.

The critical exponent δ in the ideal case might satisfy the Widom scaling relation $\delta = 1 + \gamma/\beta$ [34] which for β and γ, provided by the Arrott-Noakes analysis, gives $\delta = 3.52 \pm 0.04$. This is in excellent agreement with the value $\delta = 3.55 \pm 0.04$ obtained from direct fitting of the critical isotherm that should follow $M \sim (\mu_0 H)^{1/\delta}$. Note that the critical exponents for the mean field approximation are $\beta = 0.5$, $\gamma = 1$, and $\delta = 3$ [35]; however, we should mention the work of Yamada [36], who has shown that spin fluctuations in weak itinerant ferromagnets lead to Arrott plots linear in strong magnetic fields and bent downwards at the region of small magnetizations.

E. Paramagnetic susceptibility

The nearly identical temperature dependences of paramagnetic susceptibility measured along the [111] and [001] direction are consistent with an isotropic paramagnetic state of $U_4Ru_7Ge_6$ (see the $1/\chi$ versus T plot in Fig. 7). The susceptibility values at temperatures above 30 K can be well fitted with a modified Curie-Weiss law in the temperature range with parameters shown in Table II.

F. Heat capacity

Heat capacity data show a clear anomaly at 10.7 K as displayed in Fig. 8. This temperature is consistent with the T_C value determined from magnetization data by Arrott-Noakes plot analysis. The estimated magnetic entropy at T_C (i.e., integrated from 0.3 K to T_C) of $0.2 \cdot R \ln 2$ is much lower

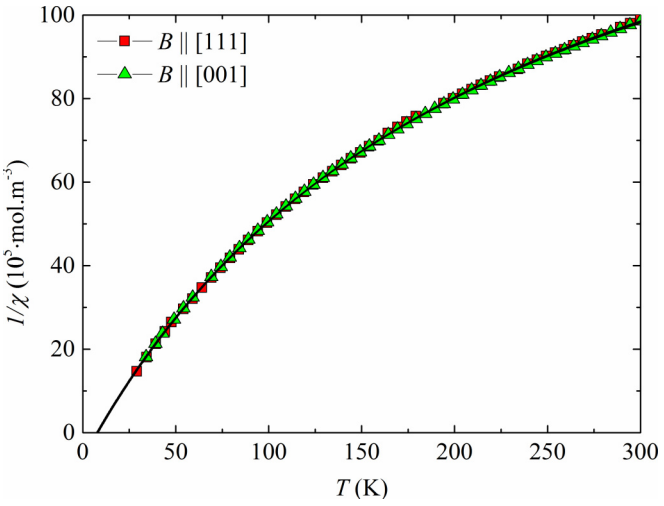

FIG. 7. Temperature dependence of the inverse susceptibility of $U_4Ru_7Ge_6$ in a magnetic field of 1 T applied along the [111] and [001] direction. The full curve represents the fit with a modified Curie-Weiss law.

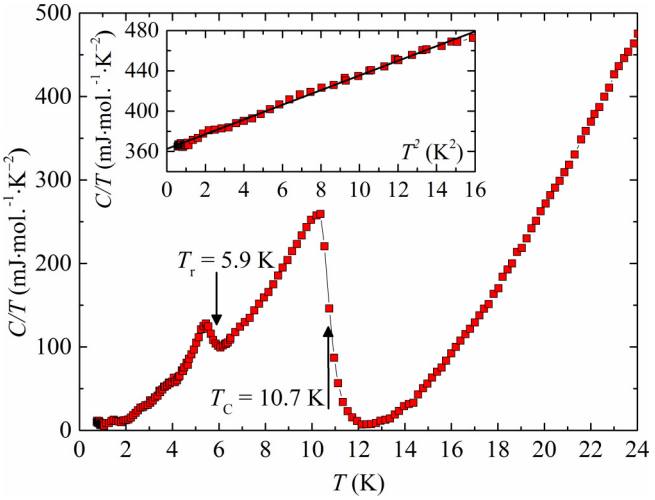

FIG. 8. Temperature dependence of the heat capacity (C/T vs T plot) of $U_4Ru_7Ge_6$. Inset: The C/T vs T^2 plot.

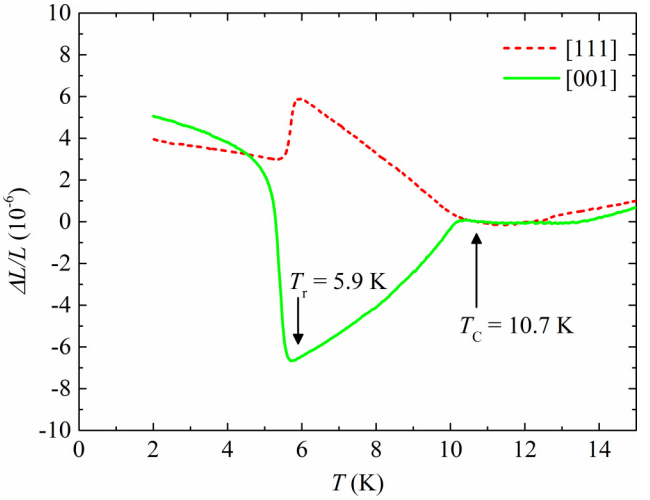

FIG. 9. Linear thermal expansion of $U_4Ru_7Ge_6$ along the [001] and [111] directions.

than R ln 2, yielding additional evidence of itinerant electron magnetism in $U_4Ru_7Ge_6$. For the itinerant limit case, in which local moments disappear at T_C, the magnetic entropy is equal to zero, because the entropy above T_C (no moments) is equal to the low-T limit (moments ordered, no fluctuations) [11]. The archetypal example of an itinerant ferromagnet is $ZrZn_2$, with entropy of $\approx 0.005\ R \ln 2$ [37,38]. The magnetic moment reorientation transition at T_r is reflected in a tiny, but clear, peak at this temperature.

The gamma coefficient of the electronic specific heat determined from a standard C/T versus T^2 plot (see inset in Fig. 8) constructed from data below 4 K is 362 mJ mol^{-1} K^{-2}. The value related to one U ion equal to 90.5 mJ mol^{-1} K^{-2} reflects the presence of the U 5f-electron states at E_F similar to numerous other U intermetallics with itinerant 5f electrons which usually exhibit elevated values somewhere between 30 and 100 mJ mol^{-1} K^{-2} per U ion.

G. Thermal expansion and magnetostriction

The linear thermal expansion $\Delta L/L$ measured along the [001] ([111]) direction in zero magnetic field (seen in Fig. 9) shows two distinct anomalies which can be attributed to the magnetic phase transitions revealed by magnetization measurements. When cooling from higher temperatures, a downturn (upturn) in the vicinity of T_C followed by a steep increase (decrease) of the corresponding $\Delta L/L$ below $\sim$6 K ($\sim T_r$) is seen for the [001] ([111]) direction, respectively.

Most thermal expansion studies of ferromagnets revealing the spontaneous magnetostriction at temperatures $T < T_C$ were done using x-ray or neutron diffraction [39]. We investigated the crystal structure of $U_4Ru_7Ge_6$ by x-ray powder diffraction at low temperatures, down to 3 K. No change of diffraction within the experimental error has been observed below 11 K.

From Fig. 9 it is, however, evident that our thermal expansion data obtained by dilatometer on the $U_4Ru_7Ge_6$ single crystal clearly demonstrate the existence of lattice distortions in the ferromagnetic state. The distortions here are, however, very small ($< 10^{-5}$).

The dilatometer enables us to determine the crystal distortions along the three perpendicular crystal axes [100], [010], and [001]. To study the corresponding linear spontaneous magnetostriction of a ferromagnet with a dilatometer one should perform measurements on a single-crystal sample containing only one ferromagnetic domain. Knowing our magnetization data, we studied the phase with the easy magnetization along [001] stable at temperatures $T_r < T < T_C$ in the following way. We first cooled the crystal down to 6.2 K (the temperature just above the onset of the spin reorientation transition) in a field of 1 T parallel to the [001] direction. At this temperature we decreased the magnetic field down to 30 mT, and then measured the thermal expansion in the longitudinal $(\Delta L/L)_{[001]}$ and transversal $(\Delta L/L)_{[100]}$ geometry with increasing temperature up to T_C. In this experiment, the thermal expansion along the c and a axis of the ferromagnetic tetragonally distorted structure was measured. A field of 30 mT applied along [001] is the minimum field maintaining the single-domain sample with the magnetic moment oriented along the c axis. These $(\Delta L/L)_{[001]}$ and $(\Delta L/L)_{[100]}$ thermal expansion data can be taken as a reasonable approximation of spontaneous linear magnetostriction (denoted as $\lambda_{S[001]}$ and $\lambda_{S[100]}$, respectively).

One can see that the value of the spontaneous tetragonal distortion is negative (the c axis shrinks) and very small ($\lambda_{S[001]} \sim -9 \times 10^{-6}$ at 6.2 K). Simultaneously the a axis expands ($\lambda_{S[100]} = \lambda_{S[010]} \sim 9 \times 10^{-6}$ at 6.2 K). Figure 10 shows also the corresponding spontaneous thermal volume expansion usually denoted as $\omega_S (= 2\lambda_{S[100]} + \lambda_{S[001]})$. As expected for an itinerant electron ferromagnet, the volume of the $U_4Ru_7Ge_6$ lattice expands below T_C. Reasonable data can be collected only down to 6.2 K. Below this temperature the magnetic-moment-reorientation transition from the [001] to the [111] direction commences; the direction of the magnetic moment becomes uncertain despite a magnetic field of 30 mT applied along [001].

H. Electrical resistivity

The almost identical corresponding values of the electrical resistivity measured for current along [111] and [001] direction

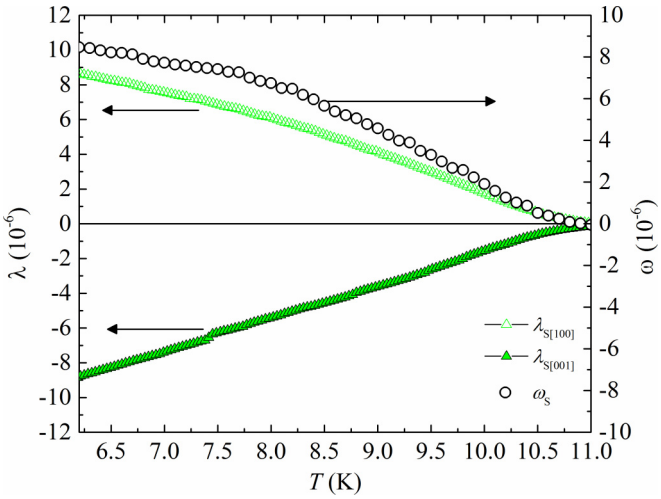

FIG. 10. Linear thermal expansion of $U_4Ru_7Ge_6$ along the [001] and [100] (denoted as $\lambda_{S[001]}$ and $\lambda_{S[100]}$ on the left axis) direction in a magnetic field of 30 mT applied along [001], and the corresponding thermal volume expansion (denoted as ω_S on the right axis). Temperatures are from 6.2 K to T_C. The data are considered as the best estimation of corresponding spontaneous magnetostriction (see text).

over the entire temperature range 2–300 K indicates a quite isotropic electron transport in $U_4Ru_7Ge_6$ (see Fig. 11). The convex $\rho(T)$ curve in the paramagnetic state resembles rather the behavior of transition-metal compounds. This trend changes at T_C to the low-temperature concave curve with a T^2 scaling. When inspecting the second derivative, we observe a deep minimum of $\partial^2\rho/\partial^2 T$ at T_C and a local minimum at T_r.

IV. DISCUSSION

The $M(\mu_0 H)$ curve measured for the hard magnetization direction [001] merges with the easy magnetization direction [111] curve near 300 mT as seen in Fig. 3. This anisotropy field of $U_4Ru_7Ge_6$ is unprecedentedly the lowest value ever

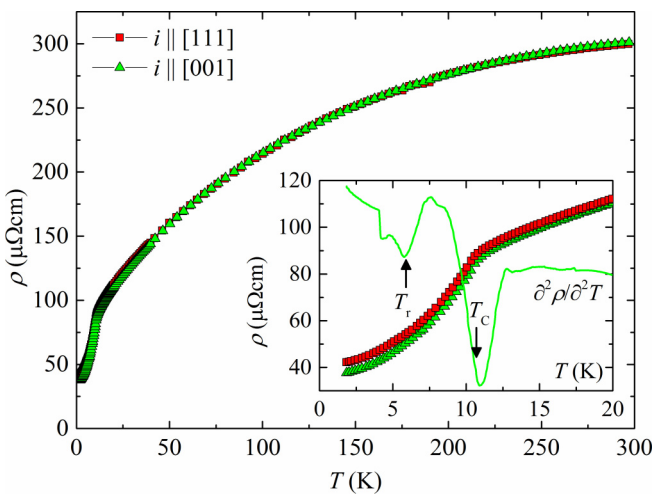

FIG. 11. Temperature dependence of electrical resistivity of the $U_4Ru_7Ge_6$ measured for current along [111] and [001] direction.

observed for a uranium intermetallic compound. Moreover, we observed an entirely isotropic paramagnetic susceptibility and electrical resistivity, which up to our best knowledge has not been reported for any uranium $5f$-electron ferromagnet.

One may argue that the almost isotropic magnetism in $U_4Ru_7Ge_6$ is a consequence of the itinerant character of U $5f$-electron magnetic moment. The spontaneous magnetic moment of this compound is $\sim 0.85\,\mu_B$/f.u., which provides an average moment of $\sim 0.21\,\mu_B$/U ion when supposing negligible contributions from Ru and Ge ions. This value is four times larger than the U-born magnetic moment of the itinerant $5f$-electron ferromagnet UNi_2 [7–10] which in contrast exhibits a huge magnetocrystalline anisotropy with the anisotropy field $\gg 35$ T [10].

Both our magnetization data and *ab initio* calculations clearly show the easy magnetization direction of $U_4Ru_7Ge_6$ in the ground state is [111]. As a result of magnetoelastic interaction [40], the ferromagnetic ordering at temperatures below T_C is accompanied by the spontaneous magnetostriction causing a distortion of a crystal lattice related to the easy magnetization direction. These distortions are present in ferromagnetic materials possessing cubic crystal structure in a paramagnetic state (at temperatures $T > T_C$). The spontaneous magnetostriction leads to a distortion lowering the paramagnetic cubic to tetragonal, orthorhombic, and rhombohedral symmetry for the [001], [110], and [111] easy magnetization directions, respectively. The expected rhombohedral distortion of the cubic $U_4Ru_7Ge_6$ lattice in the ferromagnetic ground state is so tiny that it falls within the experimental error of a standard x-ray diffraction, but is clearly indicated by thermal expansion results at low temperatures. As a consequence of the distortion, the one equivalent crystallographic site common for all U ions in the cubic lattice splits into two inequivalent ones, which is confirmed by *ab initio* calculations. Our recent experiment using polarized neutron diffraction seems to confirm this statement. Results of this experiment, after proper analysis, will be the subject of a future paper. X-ray dichroism experiments, which can deliver further complementary results needed for resolving of the two U magnetic moments issue, are desired.

Our magnetization results also reveal that the easy magnetization direction holds onto the [111] axis only at low temperatures up to T_r (=5.9 K), whereas at higher temperatures up to T_C the easy magnetization direction is unambiguously along [001] and the paramagnetic cubic lattice is tetragonally distorted along this direction. This finding is in good agreement with the theoretical calculations, which reveal the excited state with the [001] easy magnetization 0.9 meV above the ground state. The calculated total energy is the sum of positive kinetic energy and negative potential energy and negative exchange-correlation energy. The difference of kinetic energy for the [111] and [001] direction is 59.27 meV, of potential energy is −53.67 meV, and of exchange-correlation energy is −6.50 meV.

The magnetic moment reorientation transition in $U_4Ru_7Ge_6$ at T_r is manifested in specific features (anomalies) which we observed in the temperature dependencies of magnetization [Fig. 4(a)], ac susceptibility [Fig. 4(b)], specific heat (Fig. 8), thermal expansion (Fig. 9), and electrical resistivity (Fig. 11). It is in fact an order-to-order magnetic phase transition

accompanied by structural distortion due to notable magnetoelastic coupling. These phase transitions are known to be of the first-order type (e.g., $HoAl_2$ [41]). The thermal expansion anomalies seen in Fig. 9 at T_C and T_r, respectively, may be viewed as illustrative examples of the second- and first-order-type phase transitions. However, the first-order phase transition is to be accompanied by latent heat, which we were unable to detect by detailed specific-heat measurement and the T_r related specific-heat anomaly is considerably broader than expected for a first-order phase transition. We attribute the lack of observables pointing to the presence of latent heat to the complex domain structure processes during the spin reorientation in the multidomain sample in the vicinity of T_r. Crystal imperfections act as nucleation centers leading to random population of equivalent domains within a finite temperature window, effectively smearing out the latent heat contribution over a finite temperature range making it difficult to observe experimentally. Our tentative determination has to be confirmed by a designed method allowing indication of coexistence of the [001] and [111] phases in the vicinity of T_r, which would resolve the issue of the phase transition order. It might be observable in μSR spectra, in which the different signals from the [001] and [111] phase should be visible. Results that can be achieved by a μSR experiment, however, strongly depend on the actual stopping site(s) of the muon in the $U_4Ru_7Ge_6$ lattice.

The anisotropy field values in U ferromagnets are typically hundreds of Tesla, whereas in $U_4Ru_7Ge_6$ it is roughly three orders of magnitude smaller. When inspecting crystal structures we observe that in all cases of the U ferromagnets characterized by high values of anisotropy field the U ions have some U nearest neighbors. In contrast, the individual U ions in $U_4Ru_7Ge_6$ are buried inside the Ru and Ge polyhedra thereby preventing direct connection to any nearest U ion which should have consequences for magnetism [26].

The direct $5f$-$5f$ overlap of U electron orbitals is probably behind the huge magnetic anisotropy of other U compounds. The symmetry of the network of U nearest neighbors determines the type of magnetic anisotropy in these materials [11]. The very weak MA in $U_4Ru_7Ge_6$ is apparently due to the lack of the direct overlap of $5f$ wave functions of the nearest U neighbors (direct $5f$-$5f$ overlap). The symmetry of the hybridization of U $5f$-electron states with the $4d$-electron states of surrounding Ru ions, which are in a hexagonal arrangement perpendicular to the [111] axis, determines the [111] easy magnetization direction.

Onset of itinerant electron ferromagnetism is usually accompanied by a positive spontaneous magnetovolume effect [42,43]. Also our thermal expansion data show this tendency despite the negative value of $\lambda_{S[001]}$. Unfortunately, the measurements using a dilatometer cannot be extended to temperatures lower than T_r because the body diagonals representing the [111] easy magnetization direction are not perpendicular and therefore an experiment analogous to that for $T_r < T < T_C$ is not accessible.

V. CONCLUSIONS

We have grown for the first time a single crystal of $U_4Ru_7Ge_6$ and demonstrated by experiment and by SOI *ab initio* calculations the almost isotropic ferromagnetism in this compound. This result contrasts with the generally observed huge magnetocrystalline anisotropy in all the so far reported ferromagnetic uranium compounds. The ground-state easy magnetization direction is oriented along the [111] axis of the rhombohedrally distorted cubic lattice and has been found both by the experiment and the calculations. The rhombohedral distortion leads to emergence of two crystallographically inequivalent U sites. This is in agreement with results of calculations providing also different U magnetic moments at the inequivalent sites. A change of the easy magnetization direction and the symmetry of the lattice distortion have been observed experimentally at temperatures above $T_r = 5.9$ K to a tetragonal distortion and the easy magnetization along its [001], which hold for temperatures up to T_C. This finding is in accord with the calculated first exited state with the U moment along the [001] direction. The first exited state has been calculated to be 0.9 meV above the ground state, which is comparable with the value of $k_B T_r (=0.51$ meV). The spin reorientation transition at T_r is significantly projected in low-field magnetization, ac susceptibility, and thermal expansion data and causes also a weak anomaly at T_r visible in the temperature dependence of the specific heat and the electrical resistivity. The magnetoelastic interaction induces a very small rhombohedral (tetragonal) distortion of the paramagnetic cubic crystal lattice in case of the [111] ([001]) easy magnetization direction. The very weak MA found in $U_4Ru_7Ge_6$ is the most striking observation for a uranium compound. We propose that this is a consequence of a specific environment of each U ion being coordinated by the closed Ru and Ge cuboctahedral cages which are preventing the direct $5f$-$5f$ overlap, the key ingredient of the huge MA exhibited by other U magnetics.

ACKNOWLEDGMENTS

The authors are indebted to Jan Prokleška for checking the paper and providing critical insight and constructive suggestions and to M. A. Novotny for language corrections. This work was supported by the Czech Science Foundation Grant No. P204/16/06422S and by Charles University project GA UK Grant No. 720214. Experiments were performed in MLTL (http://mltl.eu/), which is supported within the program of Czech Research Infrastructures (Project No. LM2011025).

[1] F. Bloch and G. Gentile, Z. Phys. **70**, 395 (1931).
[2] J. H. van Vleck, Phys. Rev. **52**, 1178 (1937).
[3] J. F. Herbst, Rev. Mod. Phys. **63**, 819 (1991).
[4] M. D. Kuz'min and A. M. Tishin, in *Handbook of Magnetic Materials*, edited by K. H. J. Buschow (Elsevier, New York, 2007), Vol. 17, pp. 149–233.

[5] D. D. Koelling, B. D. Dunlap, and G. W. Crabtree, Phys. Rev. B **31**, 4966 (1985).

[6] M. S. S. Brooks and P. J. Kelly, Phys. Rev. Lett. **51**, 1708 (1983).

[7] V. Sechovský, Z. Smetana, G. Hilscher, E. Gratz, and H. Sassik, Physica B+C **102**, 277 (1980).

[8] J. M. Fournier, A. Boeuf, P. Frings, M. Bonnet, J. v. Boucherle, A. Delapalme, and A. Menovsky, J. Less-Common Met. **121**, 249 (1986).

[9] L. Severin, L. Nordström, M. S. S. Brooks, and B. Johansson, Phys. Rev. B **44**, 9392 (1991).

[10] P. H. Frings, J. J. M. Franse, A. Menovsky, S. Zemirli, and B. Barbara, J. Magn. Magn. Mater. **54-57**, 541 (1986).

[11] V. Sechovský and L. Havela, in *Handbook of Magnetic Materials* (Elsevier, New York, 1998), Vol. 11, pp. 1–289.

[12] G. Busch and O. Vogt, J. Less-Common Met. **62**, 335 (1978).

[13] C. F. Buhrer, J. Phys. Chem. Solids **30**, 1273 (1969).

[14] J. L. Smith and E. A. Kmetko, J. Less Common Met. **90**, 83 (1983).

[15] O. Eriksson, M. S. S. Brooks, B. Johansson, R. C. Albers, and A. M. Boring, J. Appl. Phys. **69**, 5897 (1991).

[16] V. Sechovský, L. Havela, H. Nakotte, F. R. de Boer, and E. Brück, J. Alloys Compd. **207-208**, 221 (1994).

[17] B. R. Cooper, R. Siemann, D. Yang, P. Thayamballi, and A. Banerjea, *Hybridization-Induced Anisotropy in Cerium and Actinide Systems* (North-Holland, Amsterdam, 1985).

[18] B. R. Cooper, G. J. Hu, N. Kioussis, and J. M. Wills, J. Magn. Magn. Mater. **63-64**, 121 (1987).

[19] A. A. Menovsky, J. Magn. Magn. Mater. **76-77**, 631 (1988).

[20] H. Rietveld, J. Appl. Crystallogr. **2**, 65 (1969).

[21] J. Rodriguez-Carvajal, Physica B: Condensed Matter **192**, 55 (1993).

[22] T. Roisnel and J. Rodriguez-Carvajal, in *EPDIC 7—Seventh European Powder Diffraction Conference*, edited by R. Delhez and E. Mittemeijer (Trans Tech Publications, Barcelona, Spain, 2000).

[23] M. Rotter, H. Müller, E. Gratz, M. Doerr, and M. Loewenhaupt, Rev. Sci. Instrum. **69**, 2742 (1998).

[24] B. Lloret, B. Buffat, B. Chevalier, and J. Etourneau, J. Magn. Magn. Mater. **67**, 232 (1987).

[25] S. A. M. Mentink, G. J. Nieuwenhuys, A. A. Menovsky, and J. A. Mydosh, J. Appl. Phys. **69**, 5484 (1991).

[26] S. F. Matar, B. Chevalier, and R. Pöttgen, Solid State Sci. **27**, 5 (2014).

[27] E. Du Trémolet de Lacheisserie, D. Gignoux, and M. Schlenker, *Magnetism* (Springer, New York, 2005).

[28] K. Koepernik and H. Eschrig, Phys. Rev. B **59**, 1743 (1999).

[29] J. P. Perdew and Y. Wang, Phys. Rev. B **45**, 13244 (1992).

[30] J. P. Perdew, K. Burke, and M. Ernzerhof, Phys. Rev. Lett. **77**, 3865 (1996).

[31] M. W. McElfresh, J. H. Hall, R. R. Ryan, J. L. Smith, and Z. Fisk, Acta Crystallographica C **46**, 1579 (1990).

[32] A. Arrott, Phys. Rev. **108**, 1394 (1957).

[33] A. Arrott and J. E. Noakes, Phys. Rev. Lett. **19**, 786 (1967).

[34] B. Widom, J. Chem. Phys. **43**, 3892 (1965).

[35] P. Weiss, J. Phys. Theor. Appl. **6**, 661 (1907).

[36] H. Yamada, Phys. Lett. A **55**, 235 (1975).

[37] E. P. Wohlfarth, J. Appl. Phys. **39**, 1061 (1968).

[38] R. Viswanathan, J. Phys. F **4**, L57 (1974).

[39] A. V. Andreev, in *Handbook of Magnetic Materials* (Elsevier, New York, 1995), Vol. 8, pp. 59–187.

[40] E. R. Callen and H. B. Callen, Phys. Rev. **129**, 578 (1963).

[41] P. Durga, K. P. Arjun, V. K. Pecharsky, and J. K. A. Gschneidner, J. Phys.: Condens. Matter **25**, 396002 (2013).

[42] M. Shimizu, Physica B: Condensed Matter **159**, 26 (1989).

[43] P. Mohn, K. Schwarz, and D. Wagner, Physica B: Condensed Matter **161**, 153 (1990).